

Dietary Change Enables Robust Growth-Coupling of Heterologous Methyltransferase Activity in Yeast

Anne Sofie Lærke Hansen, Maitreya J. Dunham, Dushica Arsovska, Jie Zhang, Jay D. Keasling, Markus J. Herrgard, and Michael K. Jensen*



Cite This: <https://dx.doi.org/10.1021/acssynbio.0c00348>



Read Online

ACCESS |



Metrics & More



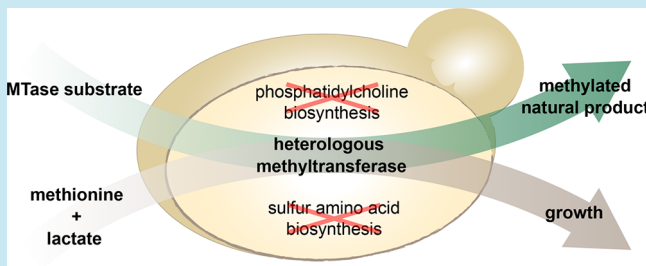
Article Recommendations



Supporting Information

ABSTRACT: Genetic modifications of living organisms and proteins are made possible by a catalogue of molecular and synthetic biology tools, yet proper screening assays for genetic variants of interest continue to lag behind. Synthetic growth-coupling (GC) of enzyme activities offers a simple, inexpensive way to track such improvements. In this follow-up study we present the optimization of a recently established GC design for screening of heterologous methyltransferases (MTases) and related pathways in the yeast *Saccharomyces cerevisiae*. Specifically, upon testing different media compositions and genetic backgrounds, improved GC of different heterologous MTase activities is obtained. Furthermore, we demonstrate the strength of the system by screening a library of catechol O-MTase variants converting protocatechuic acid into vanillic acid. We demonstrated high correlation ($R^2 = 0.775$) between vanillic acid and cell density as a proxy for MTase activity. We envision that the improved MTase GC can aid evolution-guided optimization of biobased production processes for methylated compounds with yeast in the future.

KEYWORDS: growth-coupling, methyltransferase, yeast, synthetic biology, natural products, screening



To facilitate the transition into a biobased society, a myriad of tools and strategies have been developed to engineer both proteins and microbes into biological catalysts to sustain production of natural and heterologous compounds.^{1,2} Biochemical production or enzyme activity, whether improved or established *de novo*, rarely confers a beneficial, easily selectable phenotype, yet assays and tools to screen for improved variants are needed.^{3,4} Synthetic growth-coupling (GC) offers a valuable complementary tool to other high-throughput screens depending on more advanced laboratory equipment like fluorescence-activated cell sorting or state-of-the-art analytical instrumentation,^{5,6} due to growth being a simple read-out. In addition, GC overcomes crucial bottlenecks in the current bioengineering workflow as no knowledge is needed *a priori* about the limitations underpinning the trait in question. Indeed, properly designed GC allows screening for any edit, genome-wide or targeted to defined open reading frames, giving rise to improved growth, such as recently exemplified *in silico* and experimentally for vanillin and succinic acid production, respectively.^{7,8} Despite this, the number of successful implemented GC designs are limited.⁹ Additionally, many current GC strategies only target optimization of a single enzyme or product, making the return-of-investment low regarding effort and time spent on establishing the GC design.

We have previously presented a universal GC design of SAM-dependent methyltransferases (MTases) and associated pathways in *Escherichia coli* and *Saccharomyces cerevisiae* by

taking advantage of coupled methionine and cysteine biosynthesis in sulfur amino acid auxotrophic strains.¹⁰ MTases form an abundant class (EC 2.1.1.—) of enzymes catalyzing key steps in many biosynthetic pathways toward natural products of commercial and societal interests^{11–14} and are promising biocatalysts.¹¹ Uniquely targeting a large and substrate-diverse enzyme class, our GC design allows screening for and optimization of the biosynthesis of a broad range of products *via* simple assessment of growth. In yeast, GC is only obtained when abundant competing native MTases are deleted. However, a substantial growth-leakiness is still observed in strains expressing a heterologous MTase, even without any substrate to methylate.¹⁰ Given the interest in biobased production of bioactive compounds in yeast,¹⁵ we therefore sought to improve the MTase GC.

Here we present results from our efforts to robustly growth-couple diverse heterologous MTase activities in yeast. By testing different cultivation conditions and genetic backgrounds we successfully abolish the previously observed leakiness. We then demonstrate GC of two additional

Received: June 30, 2020

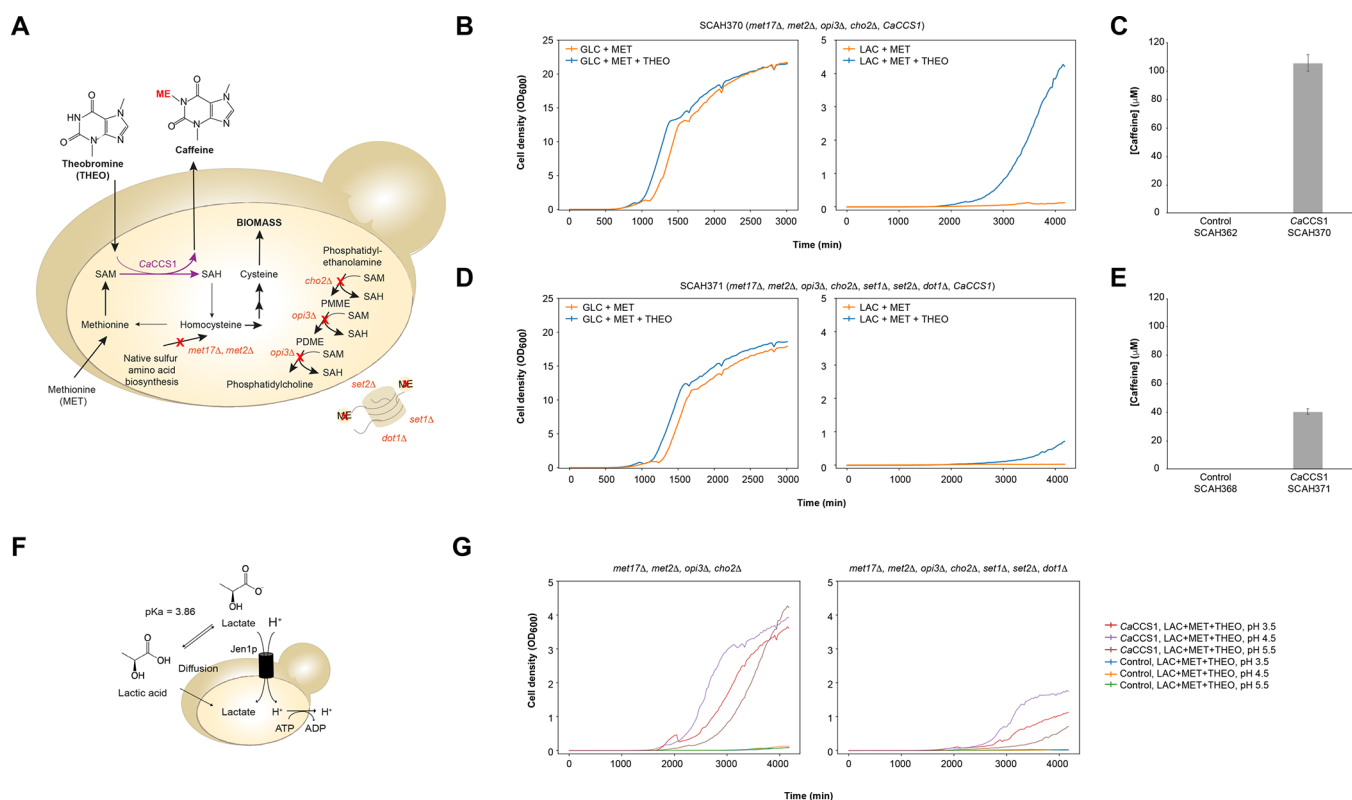


Figure 1. Design and characterization of improved MTase GC in *S. cerevisiae*. (A) MTase GC design in *S. cerevisiae* SCAH124 (*met17Δ*, *met2Δ*, *cho2Δ*, *opi3Δ*) and SCAH354 (*met17Δ*, *met2Δ*, *cho2Δ*, *opi3Δ*, *set2Δ*, *set1Δ*, *dot1Δ*). *CaCCS1* methylation reaction is colored in purple. Red crosses indicate gene deletion. Byproducts, cofactors, and substrates are left out. (B,D) Growth of MTase GC strains SCAH370 (B) and SCAH371 (D) expressing *CaCCS1* on GLC (left) and LAC (right) with MET and with (blue) and without (orange) the methyl group acceptor THEO (1 mM) (pH 5.5). (C,E) Caffeine titer for strain pairs (empty plasmid control and *CaCCS1* expressing strain), SCAH362 and SCAH370 (C), as well as SCAH368 and SCAH371 after 4776 min cultivation in LAC+MET+THEO (1 mM) medium ($n = 3$) (pH 5.5). (F) Schematic of simplified LAC uptake mechanism in *S. cerevisiae* via diffusion or permease JEN1. (G) Growth of strain pairs (empty plasmid control and *CaCCS1* expressing strain), SCAH362 and SCAH370 (left) and SCAH368 and SCAH371 (right) in LAC+MET+THEO (1 mM) medium at pH 3.5 (red and blue), 4.5 (purple and orange), and 5.5 (brown and green). Growth curves are based on data from one representative isolate ($n = 1$). Curves for three replicates in [Supplementary Figure S1](#). For all media, both MET and choline were supplemented to a final concentration of 1 mM each. Abbreviations, GLC: glucose, LAC: lactate/lactic acid, ME: methyl group, MET: methionine, THEO: theobromine, SAH: S-adenosylhomocysteine, SAM: S-adenosylmethionine, PDME: phosphatidylmethylethanolamine, PMME: phosphatidylmonomethylethanolamine.

heterologous MTases, thus adding further evidence for this robust and generic GC as a synthetic biology tool for development and identification of superior enzymes and yeast cell factories for biobased manufacturing of methylated compounds.

RESULTS AND DISCUSSION

The recently published functional MTase GC in *S. cerevisiae* consists of four gene knockouts (*S. cerevisiae* SCAH124):¹⁰ *met17Δ* and *met2Δ* for establishing sulfur amino acid auxotrophy, as well as *cho2Δ* and *opi3Δ*, encoding two endogenous MTases, to reduce native conversion capacity of SAM to S-adenosylhomocysteine (SAH) (Figure 1A).¹⁶ As *S. cerevisiae* harbors >90 endogenous MTases that make up a large intertwined genetic interaction network, the methyl-transferase,¹⁷ we speculated that the leakiness of the minimal MTase GC design was caused by the (hyper-)activity of remaining native MTases. In line with this hypothesis, it has been reported that the activity of yeast histone MTases increases in *cho2Δ* strains when cultivated in lactate-based medium.¹⁸ Accordingly, we investigated the effect on MTase GC of (1) replacing the previously applied fermentable carbon and energy source glucose with the nonfermentable alternative

lactate, and (2) deleting three histone MTases Set2p, Set1p, and Dot1p (Figure 1A).

First, we developed a simplified and more easily manageable workflow without sulfur amino acid starvation compared to the previous cultivation scheme.¹⁰ We also adjusted the medium, and left out the buffer system and excess amounts of inorganic sulfate, since the MTase GC strains can not assimilate it due to the *MET17* deletion. Both methionine and choline (to enable phosphatidylcholine synthesis) were maintained supplemented at a concentration of 1 mM. In these conditions, the modest GC of the quadruple knockout GC strain SCAH124 was recapitulated (Figure 1B). Upon expression of heterologous N-MTase caffeine synthase 1 from *Coffea arabica* (*CaCcs1p*) in the SCAH124 background (SCAH370) we observed GC of *CaCcs1p* activity on glucose in the presence of the MTase substrate theobromine (1 mM). Yet, as observed previously,¹⁰ strain SCAH370 also grew in the absence of theobromine and reached similar cell density by stationary phase compared to growth with theobromine (Figure 1B).

Next, upon replacing glucose with lactate, we observed that GC dramatically increased (Figure 1B). Indeed, in the presence of theobromine, strain SCAH370 reached approximately 35-fold higher cell density compared to growth in the

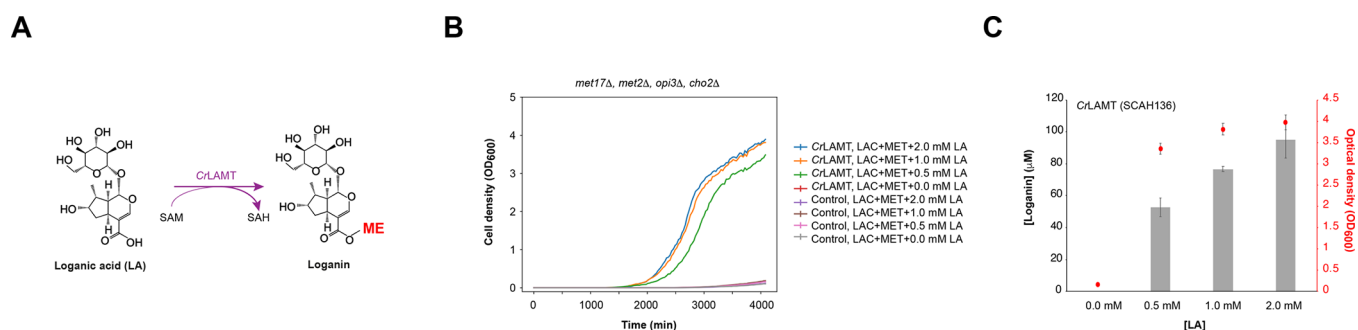


Figure 2. Investigation of CrLamtp methylation within minimal *S. cerevisiae* MTase GC strain design. (A) CrLamtp catalyzed methylation of LA into loganin. (B) Growth of MTase GC strain (*met17Δ*, *met2Δ*, *cho2Δ*, *opi3Δ*) SCAH136 expressing CrLAMT and SCAH138 with an empty plasmid in LAC+MET medium with LA concentrations 2 (blue and purple), 1 mM (orange and brown), 0.5 mM (green and pink), or no feeding (red and gray) (pH 4.55). (C) Loganin titer upon 4079 min cultivation of strain SCAH136 expressing CrLAMT in LAC+MET medium with either no, 0.5 mM, 1 mM, or 2 mM LA supplemented ($n = 3$) (pH 4.55). For all media, both MET and choline were supplemented to a final concentration of 1 mM each. Abbreviations, LA: loganic acid, ME: methyl group.

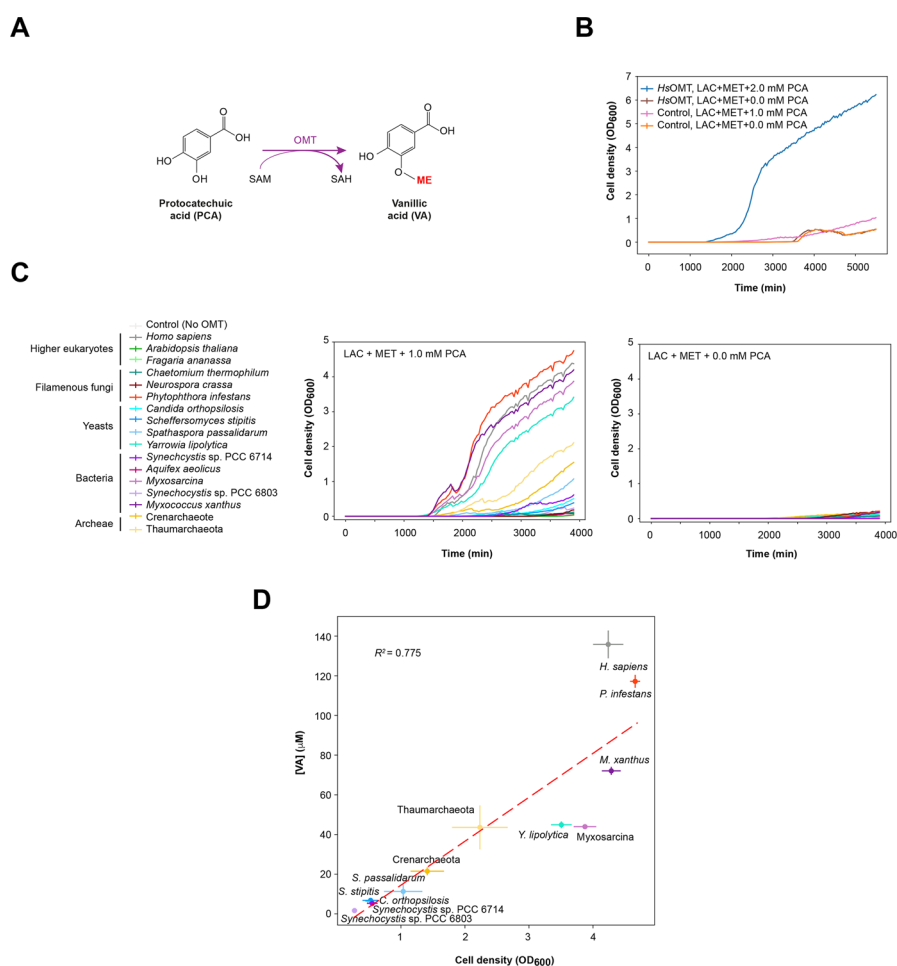


Figure 3. Semithroughput OMT variant screening using minimal *S. cerevisiae* MTase GC strain design. (A) OMT catalyzed methylation of PCA into VA. (B) Growth of MTase GC strain (*met17Δ*, *met2Δ*, *cho2Δ*, *opi3Δ*) SCAH344 expressing HsOMT from human and empty plasmid control SCAH138 in LAC+MET medium with no (brown and orange) or 1 mM PCA (blue and pink) (pH 4.3). (C) Growth of MTase GC strains expressing 17 different OMT variant genes and control strain with empty plasmid in LAC+MET medium with 1 mM PCA (left) or no feeding (right) (pH 4.3). (D) Correlation plot between of cell density (OD_{600}) on 1st axis, and VA (μM) titer on 2nd axis upon sampling after cultivation in LAC+MET+PCA (1 mM) medium for ~3900 min of the 11 OMT variants with VA production ($n = 3$, except for *Synechocystis* sp. PCC 6714 ($n = 2$), and SCAH344 ($n = 6$)). Bars represent standard deviation. Linear regression line is displayed in red. Growth curves are based on data from one representative isolate ($n = 1$). Curves for three replicates in [Supplementary Figure S1](#). Colors and nuances reflect OMT origin, archaee: yellow, bacteria: purple, filamentous fungi: red, yeasts: blue, and higher eukaryotes: green, HsOMT and empty plasmid control: gray. For all media, both MET and choline were supplemented to a final concentration of 1 mM each.

absence of theobromine ($OD_{600} = 4.19 \pm 0.21$ vs $OD_{600} = 0.12 \pm 0.03$, $n = 3$), while reaching a titer of $105.8 \pm 5.8 \mu\text{M}$ caffeine upon sampling compared to no measurable production for strain SCAH362 without *CaCcs1p* expression in lactate (Figure 1C).

Deleting the genes encoding the histone MTases *Set2p*, *Set1p*, and *Dot1p* in the SCAH124 background (SCAH354) and introducing *CaCCS1* (SCAH371) caused an increase in lag-phase and similar modest GC on glucose as observed for SCAH370 (Figure 1D). Yet, even though GC for the septuple knockout strain SCAH371 was also improved on lactate ($OD_{600} = 0.82 \pm 0.18$ with theobromine vs $OD_{600} = 0.04 \pm 0.04$ without theobromine), and a caffeine titer of $40.6 \pm 1.7 \mu\text{M}$ was observed, SCAH371 grew to lower OD_{600} compared to the quadruple knockout strain SCAH370 ($OD_{600} = 0.82 \pm 0.18$ vs $OD_{600} = 4.19 \pm 0.21$) (Figure 1D,E).

Extending from the improved GC when feeding lactate, we next sought to further investigate the effect of the cultivation medium. Lactic acid is a weak short-chain monocarboxylic acid ($pK_a = 3.86$), which in the presence of glucose passively diffuses into the cell in its undissociated form, while at the same time posing a growth-inhibitory effect on yeast among other things due to the energy-intensive mechanism for maintaining proton homeostasis^{19,20} (Figure 1F). However, in the absence of glucose, lactate is primarily imported *via* glucose-repressed permease *Jen1p*, a proton symporter^{21,22} (Figure 1F). Acknowledging the potential importance of the pH of the cultivation medium for lactate/lactic acid uptake, its growth inhibitory effect and the effect on general cell physiology of pH when feeding an acid, we investigated the effect on growth and GC of strains SCAH124 and SCAH354 transformed with either empty plasmids (SCAH362 and SCAH368) or a plasmid with *CaCCS1* (SCAH370 and SCAH371) in lactate based medium adjusted to pHs 3.5, 4.5, or 5.5 (Figure 1G). Here, the GC, as inferred by growth in medium with theobromine, was best at pH 4.5, as also observed for a wild-type *S. cerevisiae* strain grown in the same media (Figure 1G, Supplementary Figure S1). For the entire pH range, we observed clear separation between growth of strains expressing *CaCcs1p* compared to empty plasmid controls, indicating that pH of the cultivation media can be adjusted as needed without affecting GC (Figure 1G).

Taken together, we have established a significantly improved GC of the platform quadruple knockout GC strain SCAH124 expressing a heterologous MTase when feeding its substrate by replacing glucose with lactate as a carbon source. In addition, we have developed a simplified workflow enabling high-throughput screening and demonstrated that GC is functional at various pHs.

Next, we set out to confirm that the GC was applicable for other SAM-dependent MTases as well. Thus, in addition to the N-MTase *CaCcs1p*, we tested two O-MTases in MTase GC strain *S. cerevisiae* SCAH124. First, we tested the plant loganic acid O-MTase from *Catharanthus roseus* (*CrLamtp*) methylating loganic acid into loganin, a precursor for the scaffold strictosidine branching out to >2000 different monoterpene indole alkaloids, several with medicinal properties (SCAH136, Figure 2A).^{12,23} Here, feeding different concentrations of loganic acid to SCAH136 expressing *CrLamtp* enabled titratable growth with a maximum of approximately 57-fold and 25-fold higher cell densities compared to the strain without expression of *CrLamtp* (SCAH138) or loganic acid feeding (Figure 2B), respectively ($OD_{600} = 3.98 \pm 0.14$

(SCAH136) vs $OD_{600} = 0.07 \pm 0.04$ (SCAH138) in 2 mM loganic acid, and $OD_{600} = 0.16 \pm 0.02$ (SCAH136 without loganic acid)) (Figure 2B). MTase activity was confirmed to correlate with cell densities enabling loganin titers of $95.12 \pm 11.62 \mu\text{M}$ following 2.0 mM loganic acid feeding for strain SCAH136 (Figure 2C).

Next, motivated by the improvement and robustness of the yeast MTase GC, we sought to apply the GC system as a simple screening tool for MTase product formation of relevance for semithroughput workflows. For this test we first applied GC of human catechol O-MTase (*HsOmt*) activity for methylating protocatechuic acid thereby forming vanillic acid (SCAH344).²⁴ Here, feeding the *HsOMT* substrate protocatechuic acid (1 mM) to SCAH344 cultivated in lactate-based medium conferred a significant growth advantage over the absence of *HsOMT* (SCAH138) or protocatechuic acid ($OD_{600} = 6.16 \pm 0.17$, $OD_{600} = 1.01 \pm 0.02$, and $OD_{600} = 0.67 \pm 0.17$ after cultivation for 5492.25 min, $n = 3$, respectively) (Figure 3A,B). Next, we tested a library of 16 previously characterized OMT variants of different origins²⁵ (Figure 3A) together with the *HsOMT* and empty plasmid control in the SCAH124 background (SCAH138 and SCAH328-SCAH344, Figure 3C, Supplementary Table S2). The library has previously been found to possess different activities by others.²⁵ Each yeast strain expressing an OMT variant was cultivated individually in lactate-based medium with protocatechuic acid (1 mM), from which growth and vanillic acid formation was quantified. From this screen, OMT variants were observed to give rise to a range of different cell densities from 0.05 ± 0.02 to 4.66 ± 0.08 (OD_{600}), as well as vanillic acid titers from 0 to $135.8 \pm 7 \mu\text{M}$ by the end of the cultivation (Figure 3C, Supplementary Table S1). This illustrates the applicability of the system for semithroughput screening. Indeed, with a correlation coefficient of $R^2 = 0.775$ from linear regression between reached cell density and produced vanillic acid for OMT library variants possessing vanillic acid production, the system holds promise as a tool for easy discrimination of variants within large libraries (Figure 3D).

In summary, in this study a noticeable improvement of the resolution of the MTase GC of *S. cerevisiae* was obtained by simple medium optimization, with minimal leakiness (*i.e.*, residual growth) observed in the absence of either MTase substrate or MTase activity. Conversely, deletion of proposed hyperactive histone MTases did not have an impact on GC leakiness. While this study does not address the mechanism for the strengthened coupling phenotype upon change of carbon source, the effect of lactate has previously been studied in relation to sulfur amino acid and phospholipid biosynthesis.^{18,26,27} Still, lactate is an unusual carbon source known to cause stress and abnormal growth, and we therefore have also tested the more commonly applied carbon sources, galactose, glycerol, and ethanol (Supplementary Figure S2). Here, we observed that only upon addition of 0.2% glucose were the strains able to grow on the nonfermentable alternatives ethanol and glycerol. Yet, although the resolution of the GC increased when using either galactose, glycerol, and ethanol compared to using solely glucose, the alternative carbon sources also resulted in leaky growth of *S. cerevisiae* SCAH362 without MTase expression. While out of the scope for the present study, we foresee additional genetic and physiological studies in the near future to be needed in order

to understand the mechanism behind the improved GC when using lactate as a carbon source.

The results on the GC of the activity of both N- and O-type MTases in *S. cerevisiae* underlines the expected broad applicability of the GC design to any sufficiently active SAM-dependent MTase that can (i) be expressed in *S. cerevisiae*, and (ii) for which the substrate can be presented endogenously or is not lethal when fed to the cells. Upon the optimization of the GC system we also demonstrated semithroughput *in vivo* screening of MTase variants and proved correlation between titers and cell density. In the future, upon further testing and characterization it might be possible to apply the yeast MTase GC for selection within high-throughput directed evolution and ALE workflows.

Beyond their abundance in biosynthetic pathways for natural products, MTase reactions are also found in many metabolic pathways and are implicated in genetic and metabolic diseases.^{28,29} We therefore also consider this optimized GC system of relevance for biomedical purposes outside the realm of biotechnology such as the *in vivo* study of mutation effects within clinically interestingly human MTases.

METHODS

Strains, Media, and Growth Conditions. *Saccharomyces cerevisiae* CEN.PK102–5B (MATa) was used as a background strain in the study. A complete list of all yeast strains used in the study can be found in [Supplementary Table S2](#). Gene deletions were facilitated by CRISPR/Cas9,³⁰ and all yeast transformations were performed using the lithium acetate/single-stranded carrier DNA/PEG method.³¹ *S. cerevisiae* SCAH100 derived from CEN.PK102–5B carried plasmid pRS415U ([Supplementary Table S3](#)). *S. cerevisiae* SCAH354, derived from SCAH124,¹⁰ was constructed by CRISPR/Cas9-facilitated full ORF marker-free deletion mediated by homology-directed recombination of three open-reading frames (ORFs) *SET2*, *DOT1* and *SET1* using the guide-RNA (gRNA) expressing plasmids PL_01_E6 and PL_01_E3, together with plasmid PL_01_A9 with *SpCAS9* and two linear DNA fragments homologous to the up- and downstream regions flanking the targeted ORFs. The gRNA sequences were identified using the web service CRISPy adapted to the genome sequence of *S. cerevisiae* CEN.PK:³² *SET2* (5'-GAACCAAAGTGTGAGTGCG-3'), *DOT1* (5'-GGATA-TTGTAACCGTAGACA-3') and *SET1* (5'-AAGGCATAAT-TCACTCGCGT-3').

All chemicals used in the study were purchased from Sigma-Aldrich, unless otherwise stated. The basal minimal medium was modified from Boer *et al.*³³ by leaving out any inorganic sulfur source and consisted of per L: 4 g NH₄Cl, 3 g KH₂PO₄, 0.4412 g MgCl₂·6H₂O, 1 mL vitamin solution, 2 mL trace metal solution. In addition, choline chloride and L-methionine were supplemented to a final concentration to 1 mM each. As carbon sources either 2% glucose or 3% lactate (Sigma-Aldrich, W261106) were used. The trace metal solution consisted of per L: 4.5 g CaCl₂·2H₂O, 4.5 g ZnSO₄·7H₂O, 3 g FeSO₄·7H₂O, 1 g H₃BO₃, 1 g MnCl₂·4H₂O, 0.4 g Na₂MoO₄·2H₂O, 0.3 g CoCl₂·6H₂O, 0.1 g CuSO₄·5H₂O, 0.1 g KI, and 15 g EDTA. The vitamin solution consisted of per L: 50 mg biotin, 200 mg *p*-aminobenzoic acid, 1 g nicotinic acid, 1 g Ca-pantothenate, 1 g pyridoxine-HCl, 1 g thiamine-HCl, 25 mg myo-inositol. When stated, the media was supplemented with methyl acceptors protocatechuic acid (1 mM, PCA), theobromine (1 mM, THEO) or loganic acid (0.5, 1, or 2

mM, loganic acid, (Carl Roth & CO). The pH of the media was adjusted with the base sodium hydroxide and the acid hydrogen chloride, and subsequently sterilized by filtration. For the carbon source experiment, the additional carbon sources were supplemented in the following concentrations: 2% galactose, 3% glycerol, and 3% ethanol, and the media contained 14.4 g/L KH₂PO₄ functioning as a buffer system. When indicated, glucose was added to a concentration of 0.2% to promote growth.

Oligonucleotides, Synthetic Genes, and Plasmids.

Synthetic genes were commercially synthesized by Twist Biosciences and Integrated DNA Technologies, Inc. (IDT). The full sequence of the synthetic genes used in this study can be found in [Supplementary Table S4](#). The OMT variant sequences of plasmid PL_02_F3-PL_02_G9 were codon optimized for *S. cerevisiae* in this study using the IDT algorithm.

Plasmid DNA assemblies were performed following the EasyClone method.³⁴ Plasmids were propagated in *E. coli* DH5α using 100 mg/L ampicillin. A full list of plasmids used can be found in [Supplementary Table S3](#).

Cultivations. For plate-based cultivations, precultures from three to six biological replicates per strain were performed in 96-round-bottom deep well plates at 30 °C/300 rpm in a total volume of 500 μL for approximately 24–28 h in synthetic complete medium without appropriate amino acids supplemented, and with 1 mM choline chloride. The precultures were diluted (inoculum) in sterile Milli-Q H₂O (30 μL culture in 470 μL Milli-Q H₂O) prior to inoculation.

Growth was recorded in a Growth Profiler 960 (System Duetz, EnzyScreen, Heemstede, The Netherlands) (GP960) using 96-flat bottom microtiter plates sealed with a gas permeable sandwich cover (EnzyScreen, Heemstede, The Netherlands). GP960 based cultivations were performed in a total volume of 250 μL including 10 μL inoculum at 30 °C/250 rpm. Growth was monitored at 30 min intervals by image scanning with GP960. On the basis of each image scan, integrated green values (G-values) for every well were light calibrated to account for position effects and converted into equivalent OD₆₀₀ values using a Monod function: $G\text{-value} = (a \cdot OD_{600}) / (b + OD_{600})$. The parameters *a*, 0.000566, and *b*, 2.202869, were determined by nonlinear regression using averaged G-values for every plate position of the GP960 of a dilution series of known OD₆₀₀ values of a culture of strain *S. cerevisiae* SCAH100. Strain SCAH100 was grown overnight in the minimal medium described earlier, but with 14.4 g/L KH₂PO₄, 1 mM THEO and 1 mM choline chloride as well as 2% glucose. The dilution series consisted of a medium blank, and seven OD₆₀₀ values from 0.08 to 24.7 (OD₆₀₀) in duplicate. All cell density values (OD₆₀₀) have been subtracted blank values.

Sampling of cultivation broth for chemical analysis was done after cultivation for 4776.5 min for strains SCAH362, SCAH368, SCAH370, and SCAH371, after 4079.25 min for strain SCAH136, and after 3899.5 min for strains SCAH138 and SCAH328-SCAH344. Cultivation of strain SCAH138 and SCAH344 for growth comparison was ended after 5492.25 min. For the carbon source experiments both with and without glucose addition, the data set was reduced to 5010.25 min for strains SCAH362 and SCAH370.

Chemical Analyses. Samples for quantification of secreted vanillic acid were prepared by mixing 190 μL cultivation broth and 190 μL absolute ethanol carefully in a 96-round-bottom

deepwell plate, centrifuged at 4000 rpm for 2 min at 4 °C, and supernatant was transferred to a multiwell plate, sealed and stored at −20 °C until further analysis. For caffeine, the cultures were centrifuged in 96-round-bottom deepwell plates at 4000 rpm for 2 min at room temperature, and 190 μ L supernatant was carefully transferred to a multiwell plate and stored similarly to vanillic acid samples. Both vanillic acid and caffeine was quantified by HPLC on a Dionex Ultimate 3000 system (Thermo Fisher Scientific) with a Supelco Discovery HS G5–3 HPLC column (150 \times 2.1 mm \times 3 μ M) (Sigma-Aldrich) held at 30 °C. For both compounds, a gradient of A, 10 mM ammonium formate, pH 3; and B, acetonitrile, at a constant flow rate of 0.7 mL/min was used as mobile phase. The elution profile for both vanillic acid and caffeine was as follows: 5% B, 0.5 min; 5% B to 60% B, 5 min; 60% B to 90% B, 0.5 min; 90% B, 2 min; 90% B to 5% B, 2 min (total 10 min/sample). Quantification against external standards diluted in medium without methyl acceptor substrate was performed using a DAD-3000 diode array detector at a wavelength of 277 nm (UV_Vis2) and a sample size of 10 μ L was injected for both vanillic acid and caffeine.

Samples for quantification of loganin production were prepared by mixing 200 μ L cultivation broth with 20 μ L 250 mg/L caffeine (internal standard) carefully in a 96-well flat bottom microtiter plate, 200 μ L was transferred to a filter plate (96-well, for multiplexing, AcroPrep Advance from VWR), and centrifuged twice at 2000 rpm for 30 s into a multiwell plate, sealed and stored similar to vanillic acid and caffeine samples. Data were acquired on an Advance UHPLC system (Bruker Daltonics, Fremont, CA, USA) equipped with a binary pump, degasser and PAL HTC-xt autosampler (CTC Analytics AG, Switzerland) coupled to an EVOQ Elite triple quadrupole MS (Bruker Daltonics, Fremont, CA, USA). The system was operated with MS Workstation 8.2.1 software (Bruker Daltonics, Fremont, CA, USA). The analytical column was a 100 mm C18 Acquity UPLC HSS T3 column 100 Å, 1.8 μ m particle size, 2.1 mm i.d. (Waters, Milford, MA, USA) with a KrudKatcher, HPLC in-line column filter, 0.5 μ m \times 0.004 in i.d. (Phenomenex, Torrance, CA, USA). The column oven temperature was set to 35 °C with an injection volume of 1 μ L and a 2 μ L injection loop. The mobile phase consisted of 0.1% formic acid (FA) in Milli-Q (solvent A) and 0.1% FA in acetonitrile (solvent B), delivered at a constant flow rate of 0.5 mL/min. The mobile phase gradient profile was as follows: starting condition 5% eluent B; 0.0–0.5 min, 5% B; 0.5–3.0 min, 5% B to 60% B; 3.0–4.0 min, 60% B to 90% B; 4.0–5.0 min, 90% B; 5.0–5.3 min, 90% B to 5% B; 5.3–7.4 min, 5% B. Acquisition was carried out using electrospray ionization operated in positive ion mode. The following parameters were used to acquire Multiple Reaction Monitoring (MRM) data: spray voltage, 4.5 kV; cone temperature, 350 °C; cone gas flow, 20; probe gas flow, 50; nebulizer gas flow, 50; heated probe temperature, 300 °C; exhaust gas, on; CID, 1.5 mTorr. The MRM scan time was set to 30 ms with standard resolution for all transitions. The collision energy was optimized for each transition. Analyte stock solutions were prepared in 0.1% FA and diluted with 0.1% FA for eight calibration levels. Data analysis was performed in Thermo Xcalibur (version 3.0.63). Caffeine was added as an internal standard before injection to both samples and calibration standards.

Blank values were subtracted from all reported product concentrations. The linear regression algorithm within the python subpackage `scipy.stats` (of the python ecosystem

SciPy³⁵ was used for calculation of the linear regression and the reported R^2 value. Only OMT variant strains with vanillic acid production has been included in the calculations, and an outlier of SCAH342 (−#1) has been excluded.

■ ASSOCIATED CONTENT

Supporting Information

The Supporting Information is available free of charge at <https://pubs.acs.org/doi/10.1021/acssynbio.0c00348>.

Table S1: Mean vanillic acid (VA) concentrations and optical densities (OD600) for yeast strains expressing OMT variants after cultivation for ~3,900 min in LAC +MET+PCA medium ($n = 3$, except for SCAH342 (*Synechocystis* sp. PCC 6714) where $n = 2$, as well as SCAH344 (Human) and SCAH138 (empty plasmid) where $n = 6$); Table S2: Strains of *S. cerevisiae* used in study; Table S3: List of plasmids used in the study; Table S4: List of MTase sequences (originally ordered as synthetic gBlock sequences); Figure S1: Growth curves for three isolates (−#1, −#2, and −#3) of different strains with and without heterologous MTase cultivated in different growth media; Figure S2: Growth curves for three isolates (−#1, −#2, and −#3) of strains *S. cerevisiae* SCAH362 and SCAH370 in media (pH 4.5) with THEO, choline chloride, and MET as well as fermentable carbon sources (PDF)

■ AUTHOR INFORMATION

Corresponding Author

Michael K. Jensen – Novo Nordisk Foundation Center for Biosustainability, Technical University of Denmark, 2800 Kgs. Lyngby, Denmark; orcid.org/0000-0001-7574-4707; Phone: +45 6128 4850; Email: mije@biosustain.dtu.dk; Fax: +45 4525 8001

Authors

Anne Sofie Lærke Hansen – Novo Nordisk Foundation Center for Biosustainability, Technical University of Denmark, 2800 Kgs. Lyngby, Denmark

Maitreya J. Dunham – Department of Genome Sciences, University of Washington, Seattle, Washington 98195, United States

Dushica Arsovska – Novo Nordisk Foundation Center for Biosustainability, Technical University of Denmark, 2800 Kgs. Lyngby, Denmark

Jie Zhang – Novo Nordisk Foundation Center for Biosustainability, Technical University of Denmark, 2800 Kgs. Lyngby, Denmark

Jay D. Keasling – Novo Nordisk Foundation Center for Biosustainability, Technical University of Denmark, 2800 Kgs. Lyngby, Denmark; Joint BioEnergy Institute, Emeryville, California 94608, United States; Biological Systems and Engineering Division, Lawrence Berkeley National Laboratory, Berkeley, California 94720, United States; Department of Chemical and Biomolecular Engineering & Department of Bioengineering, University of California, Berkeley, California 94720, United States; Center for Synthetic Biochemistry, Institute for Synthetic Biology, Shenzhen Institutes of Advanced Technologies, Shenzhen 518055, China

Markus J. Herrgard – Novo Nordisk Foundation Center for Biosustainability, Technical University of Denmark, 2800

Kgs. Lyngby, Denmark; BioInnovation Institute, 2200 Copenhagen, Denmark

Complete contact information is available at:

<https://pubs.acs.org/10.1021/acssynbio.0c00348>

Author Contributions

A.S.L.H., M.H., J.D.K., M.D., and M.K.J. conceived the study. A.S.L.H. and D.A. conducted all experimental work related to strain designs, plasmid and strain constructions and cultivations. A.S.L.H. and J.Z. analyzed data. A.S.L.H. and M.K.J. wrote the manuscript.

Notes

The authors declare the following competing financial interest(s): A.S.L.H. has filed a patent application covering the design of the GC system (EP3504318A1). J.D.K. has a financial interest in Amyris, Lygos, Demetrix, Maple Bio, Napigen, and Apertor Laboratories. The authors declare that they have no other competing interests.

ACKNOWLEDGMENTS

The authors would like to thank Lars Schrübbers, Mette Kristensen, Sarah Dina Blomquist, and Lars Boje Petersen for technical support related to chemical analyses, as well as Konrad Viehring, Robert Mans, and Lea G. Hansen for caffeine, vanillic acid, and loganin standards, respectively. We thank Suresh Surdasan for help on work with the growth profiler. The work was supported by The Novo Nordisk Foundation, and the European Union's Horizon 2020 Research and Innovation Programme under Grant Agreement No. 814645 (MIAMI). The research of M.J.D. was supported in part by a Faculty Scholar grant from the Howard Hughes Medical Institute.

REFERENCES

- (1) Becker, J., and Wittmann, C. (2018) From Systems Biology to Metabolically Engineered Cells—an Omics Perspective on the Development of Industrial Microbes. *Curr. Opin. Microbiol.* 45, 180–188.
- (2) Galanie, S., Entwistle, D., and Lalonde, J. (2020) Engineering Biosynthetic Enzymes for Industrial Natural Product Synthesis. *Nat. Prod. Rep.* 37, 1122.
- (3) Dietrich, J. A., McKee, A. E., and Keasling, J. D. (2010) High-Throughput Metabolic Engineering: Advances in Small-Molecule Screening and Selection. *Annu. Rev. Biochem.* 79, 563–590.
- (4) Zeng, W., Guo, L., Xu, S., Chen, J., and Zhou, J. (2020) High-Throughput Screening Technology in Industrial Biotechnology. *Trends Biotechnol.* 38, 888.
- (5) Taki, K., Noda, S., Hayashi, Y., Tsuchihashi, H., Ishii, A., and Zaitzu, K. (2020) A Preliminary Study of Rapid-Fire High-Throughput Metabolite Analysis Using Nano-Flow injection/Q-TOFMS. *Anal. Bioanal. Chem.* 412, 4127.
- (6) Flachbart, L. K., Sokolowsky, S., and Marienhagen, J. (2019) Displaced by Deceivers: Prevention of Biosensor Cross-Talk Is Pivotal for Successful Biosensor-Based High-Throughput Screening Campaigns. *ACS Synth. Biol.* 8 (8), 1847–1857.
- (7) Jouhten, P., Boruta, T., Andrejev, S., Pereira, F., Rocha, I., and Patil, K. R. (2016) Yeast Metabolic Chassis Designs for Diverse Biotechnological Products. *Sci. Rep.* 6, 29694.
- (8) Otero, J. M., Cimini, D., Patil, K. R., Poulsen, S. G., Olsson, L., and Nielsen, J. (2013) Industrial Systems Biology of *Saccharomyces Cerevisiae* Enables Novel Succinic Acid Cell Factory. *PLoS One* 8 (1), e54144.
- (9) Shepelin, D., Hansen, A. S. L., Lennen, R., Luo, H., and Herrgård, M. J. (2018) Selecting the Best: Evolutionary Engineering of Chemical Production in Microbes. *Genes* 9 (5), 249.
- (10) Luo, H., Hansen, A. S. L., Yang, L., Schneider, K., Kristensen, M., Christensen, U., Christensen, H. B., Du, B., Özdemir, E., Feist, A. M., Keasling, J. D., Jensen, M. K., Herrgård, M. J., and Palsson, B. O. (2019) Coupling S-Adenosylmethionine-Dependent Methylation to Growth: Design and Uses. *PLoS Biol.* 17 (3), e2007050.
- (11) Struck, A.-W., Thompson, M. L., Wong, L. S., and Micklefield, J. (2012) S-Adenosyl-Methionine-Dependent Methyltransferases: Highly Versatile Enzymes in Biocatalysis, Biosynthesis and Other Biotechnological Applications. *ChemBioChem* 13 (18), 2642–2655.
- (12) Brown, S., Clastre, M., Courdavault, V., and O'Connor, S. E. (2015) De Novo Production of the Plant-Derived Alkaloid Strictosidine in Yeast. *Proc. Natl. Acad. Sci. U. S. A.* 112 (11), 3205–3210.
- (13) Galanie, S., Thodey, K., Trenchard, I. J., Filsinger Interrante, M., and Smolke, C. D. (2015) Complete Biosynthesis of Opioids in Yeast. *Science* 349 (6252), 1095–1100.
- (14) Milne, N., Thomsen, P., Mølgaard Knudsen, N., Rubaszka, P., Kristensen, M., and Borodina, I. (2020) Metabolic Engineering of *Saccharomyces Cerevisiae* for the de Novo Production of Psilocybin and Related Tryptamine Derivatives. *Metab. Eng.* 60, 25–36.
- (15) Rahmat, E., and Kang, Y. (2020) Yeast Metabolic Engineering for the Production of Pharmaceutically Important Secondary Metabolites. *Appl. Microbiol. Biotechnol.* 104, 4659.
- (16) Sadhu, M. J., Moresco, J. J., Zimmer, A. D., Yates, J. R., 3rd, and Rine, J. (2014) Multiple Inputs Control Sulfur-Containing Amino Acid Synthesis in *Saccharomyces Cerevisiae*. *Mol. Biol. Cell* 25 (10), 1653–1665.
- (17) Gaever, G., Lissina, E., and Nislow, C. (2019) Network Dynamics of the Yeast Methyltransferome. *Microb. Cell Fact.* 6 (8), 356–369.
- (18) Ye, C., Sutter, B. M., Wang, Y., Kuang, Z., and Tu, B. P. (2017) A Metabolic Function for Phospholipid and Histone Methylation. *Mol. Cell* 66 (2), 180–193.
- (19) Narendranath, N. V., Thomas, K. C., and Ingledew, W. M. (2001) Effects of Acetic Acid and Lactic Acid on the Growth of *Saccharomyces Cerevisiae* in a Minimal Medium. *J. Ind. Microbiol. Biotechnol.* 26 (3), 171–177.
- (20) Zhou, J., Liu, L., and Chen, J. (2011) Improved ATP Supply Enhances Acid Tolerance of *Candida Glabrata* during Pyruvic Acid Production. *J. Appl. Microbiol.* 110 (1), 44–53.
- (21) Cássio, F., Leão, C., and van Uden, N. (1987) Transport of Lactate and Other Short-Chain Monocarboxylates in the Yeast *Saccharomyces Cerevisiae*. *Appl. Environ. Microbiol.* 53 (3), 509–513.
- (22) Casal, M., Paiva, S., Andrade, R. P., Gancedo, C., and Leão, C. (1999) The Lactate-Proton Symport of *Saccharomyces Cerevisiae* Is Encoded by JEN1. *J. Bacteriol.* 181 (8), 2620–2623.
- (23) Murata, J., Roepke, J., Gordon, H., and De Luca, V. (2008) The Leaf Epidermome of *Catharanthus Roseus* Reveals Its Biochemical Specialization. *Plant Cell* 20 (3), 524–542.
- (24) Lautala, P., Ulmanen, I., and Taskinen, J. (2001) Molecular Mechanisms Controlling the Rate and Specificity of Catechol O-Methylation by Human Soluble Catechol O-Methyltransferase. *Mol. Pharmacol.* 59 (2), 393–402.
- (25) Kunjapur, A. M., and Prather, K. L. J. (2019) Development of a Vanillate Biosensor for the Vanillin Biosynthesis Pathway in *E. Coli*. *ACS Synth. Biol.* 8 (9), 1958–1967.
- (26) Boumann, H. A., Gubbens, J., Koorengel, M. C., Oh, C.-S., Martin, C. E., Heck, A. J. R., Patton-Vogt, J., Henry, S. A., de Kruijff, B., and de Kroon, A. I. P. M. (2006) Depletion of Phosphatidylcholine in Yeast Induces Shortening and Increased Saturation of the Lipid Acyl Chains: Evidence for Regulation of Intrinsic Membrane Curvature in a Eukaryote. *Mol. Biol. Cell* 17 (2), 1006–1017.
- (27) Dato, L., Berterame, N. M., Ricci, M. A., Paganoni, P., Palmieri, L., Porro, D., and Branduardi, P. (2014) Changes in SAM2 Expression Affect Lactic Acid Tolerance and Lactic Acid Production in *Saccharomyces Cerevisiae*. *Microb. Cell Fact.* 13, 147.
- (28) Zhang, Y., Chen, M., Chen, J., Wu, Z., Yu, S., Fang, Y., and Zhang, C. (2014) Metabolic Syndrome in Patients Taking Clozapine:

Prevalence and Influence of Catechol-O-Methyltransferase Genotype. *Psychopharmacology* 231 (10), 2211–2218.

(29) Hall, K. T., Loscalzo, J., and Kaptchuk, T. J. (2019) Systems Pharmacogenomics - Gene, Disease, Drug and Placebo Interactions: A Case Study in COMT. *Pharmacogenomics* 20 (7), 529–551.

(30) DiCarlo, J. E., Norville, J. E., Mali, P., Rios, X., Aach, J., and Church, G. M. (2013) Genome Engineering in *Saccharomyces Cerevisiae* Using CRISPR-Cas Systems. *Nucleic Acids Res.* 41 (7), 4336–4343.

(31) Gietz, R. D., and Schiestl, R. H. (2007) Quick and Easy Yeast Transformation Using the LiAc/SS Carrier DNA/PEG Method. *Nat. Protoc.* 2 (1), 35–37.

(32) Ronda, C., Pedersen, L. E., Hansen, H. G., Kallehauge, T. B., Betenbaugh, M. J., Nielsen, A. T., and Kildegaard, H. F. (2014) Accelerating Genome Editing in CHO Cells Using CRISPR Cas9 and CRISPy, a Web-Based Target Finding Tool. *Biotechnol. Bioeng.* 111, 1604.

(33) Boer, V. M., de Winde, J. H., Pronk, J. T., and Piper, M. D. W. (2003) The Genome-Wide Transcriptional Responses of *Saccharomyces Cerevisiae* Grown on Glucose in Aerobic Chemostat Cultures Limited for Carbon, Nitrogen, Phosphorus, or Sulfur. *J. Biol. Chem.* 278 (5), 3265–3274.

(34) Jensen, N. B., Strucko, T., Kildegaard, K. R., David, F., Maury, J., Mortensen, U. H., Forster, J., Nielsen, J., and Borodina, I. (2014) EasyClone: Method for Iterative Chromosomal Integration of Multiple Genes in *Saccharomyces Cerevisiae*. *FEMS Yeast Res.* 14 (2), 238–248.

(35) Virtanen, P., Gommers, R., Oliphant, T. E., Haberland, M., Reddy, T., Cournapeau, D., Burovski, E., Peterson, P., Weckesser, W., Bright, J., van der Walt, S. J., Brett, M., Wilson, J., Millman, K. J., Mayorov, N., Nelson, A. R. J., Jones, E., Kern, R., Larson, E., Carey, C. J., Polat, İ., Feng, Y., Moore, E. W., VanderPlas, J., Laxalde, D., Perktold, J., Cimrman, R., Henriksen, I., Quintero, E. A., Harris, C. R., Archibald, A. M., Ribeiro, A. H., Pedregosa, F., and van Mulbregt, P. (2020) SciPy 1.0 Contributors. SciPy 1.0: Fundamental Algorithms for Scientific Computing in Python. *Nat. Methods* 17 (3), 261–272.